PHYSICAL REVIEW B VOLUME 49, NUMBER 4 15 JANUARY 1994-II

Electronic and magnetic properties of the spinel semiconductor $CdCr_2Se_4$

Alessandra Continenza
Dipartimento di Fisica, Università dell'Aquila, L'Aquila, Italy

Teresa de Pascale and Franco Meloni
Dipartimento di Scienze Fisiche, Università di Cagliari, Cagliari, Italy

Marina Serra
Istituto di Fisica Superiore, Università di Cagliari, Cagliari, Italy

(Received 29 April 1993; revised manuscript received 22 September 1993)

We present a first-principles study of the electronic and magnetic properties of the chromium spinel $CdCr_2Se_4$, a ferromagnetic semiconductor, which, for its interesting magnetic and electric properties has been the object of many experimental studies. Using calculations based on the full-potential linearized augmented plane wave relativistic scheme we are able to reproduce the structural equilibrium properties and to explain many of the features measured by resonant photoemission spectroscopy. In particular, we analyze the contribution of the Cr 3*d* electrons in a density-of-states study including the two spin orientations and a comparison with the binary analog CdSe.

INTRODUCTION

Ternary compounds have attracted attention in the last twenty years since their properties can be tailored for various technological devices.[1] The presence of two different cations and the wide range of possible solid solutions allows the existence of many stoichiometrically stable compounds presenting a set of predetermined physical properties.[2] Moreover, many different structural phases are allowed by the very small cohesive energy differences that make almost degenerate different crystallographic configurations.[3] The degree of freedom in synthesizing crystals with well-defined physical properties appears in this way augmented with respect to the traditional binary compounds. The interest is further increased by the difficulties related to a theoretical understanding of their structural and electronic properties. The unit cell, for example, is larger than that of the corresponding binary analogs for the need to accommodate many different atomic species. The corresponding lowering of the symmetry increases as a first consequence the computational effort necessary to obtain unambiguous results even if the resulting smaller Brillouin zone allows for the use of a reduced set of special k points. Nevertheless, computational difficulties are hindering less the study of complex systems where the role played by different atoms and structures is responsible for physical effects that may give useful hints in the study of other and more complex materials (e.g., high-T_c superconductors, ternary ferroelectrics, and intercalates).

Among the ternary compounds, spinels have been the object of extensive investigations for their unusual optical, electrical, and magnetic properties.[4] Their general formula $A^{\mathrm{II}}B_2^{\mathrm{III}}X_4^{\mathrm{VI}}$ favors the existence of a number of different arrangements where the X anions are generally O, S, Se, and Te. In these compounds the anions form typically a slightly distorted cubic close-packed lattice into whose tetrahedral and octahedral holes the cations are variously arranged. The distortion, which is considered the peculiar crystallographic characteristic of this class of materials, is produced by the combined effect of different cations and ordered arrays of vacant sites.[5] Spinels are defined normal when only divalent atoms occupy tetrahedral sites. Inverse spinels, on the contrary, are characterized by an exchange between the two kinds of cations; the degree of inversion, ranging continuously from zero to one, is defined as the percentage of the divalent atom which are exchanged. As a consequence, since all the octahedral sites are crystallographically equivalent, the inverse spinels are intrinsically disordered. Previous studies performed within the first-principles, norm-conserving self-consistent pseudopotential method have pointed out the difficulties in exactly defining the energy differences for various degrees of normality for the $MgIn_2S_4$ crystal.[4]

In particular it has been shown that not only the energy differences depend dramatically on the lattice relaxation, but so also does the relative order of the inverse and partially inverse structures. As a general consequence of the great degree of freedom allowed by the complexity of the ternary structure, spinels undergo various phase transitions with pressure. A study of this kind has been performed on the quasicubic $CdIn_2Se_4$ reproducing in the pseudopotential scheme the transition pressure of 10 kbar that brings the structure to crystallize in the spinal configuration.[6] All electron studies have considered the problem of the vacant sites in this class of materials with particular attention on the effects due to the anion relaxation on the structural properties.[7] Another reason for interest is related to the wide range of magnetic experimental studies that, until now, have been poorly supported by reliable theoretical calculations. The computational difficulties are mainly due to the inclusion of transition elements in the study. Experiments range from the first old investigations on the magnetoabsorption in chalcogenide spinels[8] to the recent interpretation of their

0163-1829/94/49(4)/2503(6)/$06.00

anomalous negative magnetoresistance with the aid of semiempirical models.[9]

In this paper we discuss the results obtained from the *ab initio* relativistic full-potential linearized augmented plane-wave method[10] giving particular attention to the electronic charge densities and to the projected density of states in the two different spin orientations for the magnetic spinel $CdCr_2Se_4$; our results are then compared to photoemission results.[9,11]

The ferromagnetic order in this compound is defined at 130 K (Ref. 12) and shows a strong interaction between carriers and spins. We present a study which is able to give a well-defined comparison between experiment and the results obtained with the help of non-first-principles calculations.[9,13]

Section I will describe the crystallographic structure and some details of the method. Section II will report the results for the paramagnetic and ferromagnetic phases with a discussion. In the Conclusions we will point out the state of the study together with some future prospectives.

I. STRUCTURE AND METHOD

We performed band-structure calculations for the equilibrium crystal configuration of the spinel-type $CdCr_2Se_4$. The symmetry of the crystal is cubic, space group O_h^7 ($Fd3m$), and the unit cell contains 14 atoms whose lattice positions are reported elsewhere.[4] When the value of the so-called *internal distortion parameter u* is $\frac{3}{8}$, the anions lie on an ideal fcc lattice: in this case all the Cr atoms are located in octahedral sites and all the Cd ones in tetrahedral sites. The undistorted configuration of $CdCr_2Se_4$ in the normal phase is depicted in Fig. 1.

All-electron full-potential linearized augmented plane wave[10] (FLAPW) calculations have been used within the local-density approximation (LDA). We calculated the paramagnetic as well as the ferromagnetic state; for the paramagnetic state we used the Hedin and Lundqvist[14] form for the exchange-correlation potential while for the ferromagnetic state, within the spin-polarized scheme, we used the parametrization by von Barth and Hedin.[15] In both calculations, the experimental values[13] for the lattice constant and the internal distortion parameter u ($a = 10.721$ Å and $u = 0.383$) were used.

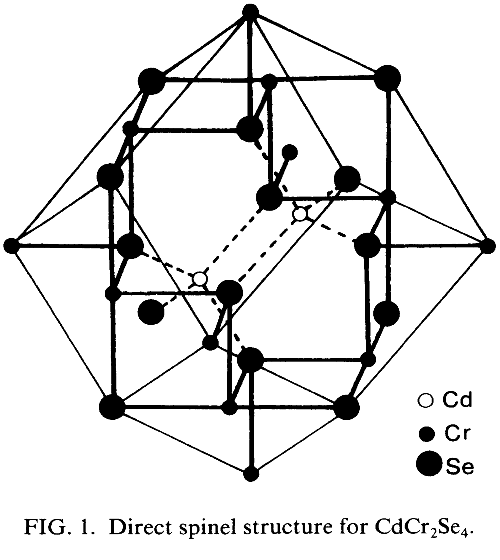

FIG. 1. Direct spinel structure for $CdCr_2Se_4$.

In the FLAPW scheme the core states are calculated fully relativistically and updated at each iteration, whereas for the valence states a semirelativistic calculation is performed; the effect of spin-orbit coupling on the energy bands is considered as a perturbation on the semirelativistic calculation. We also considered the effect of spin-orbit coupling on the spin-polarized calculation, using a second variation scheme.[16]

In the present calculation, the outermost d states of Cd are considered as part of the valence bands, since they are quite shallow in energy (see discussion later). The Se $3d$ orbitals, on the other hand, are considered as (self-consistently updated) core states, and the ~ 0.18 electrons spilling out of the muffin-tin sphere are treated by means of the overlapping charge method.[17] Inside the muffin-tin spheres, the wave function is expanded in spherical harmonics up to $l_{max} = 8$, while $l_{max} = 6$ is used for the charge density and the potential expansions. Integrations over the irreducible wedge of the Brillouin zone was performed using 10 special k points.[18] Convergency with respect to the number of k points used to integrate the charge density, was checked by using also the linear tetrahedron method[19] with a mesh of up to 80 k points. The difference in the converged charge density occupation was of the order of 0.01 electron. The muffin-tin radii used were $R = 2.3$ a.u. for all the elements and convergency was achieved using a cutoff $RK_{max} = 7.2$.

II. RESULTS AND DISCUSSION

A. Paramagnetic calculation

In Fig. 2(a) we show the calculated total density of states (DOS) obtained from the paramagnetic calculation.

At very low energies, below the Fermi level, we find the well localized $5s$ states of the Se (-14.0 eV not shown in the figure) and the $4d$ states of the cation (Cd) weakly hybridized with the Se s states. The main body of the valence band (between -7.5 eV and the Fermi level) is constituted by the d states of Cr and the p bonding states of Se.

The presence of a high peak on top of the Fermi level shows clearly that the nonmagnetic phase is highly unstable, even within the simplified picture of the Stoner criterion. It is interesting to remark that the major contribution to this peak comes from the d states of Cr, the Fermi level laying in the middle of these states. The Cr d band extends also above the Fermi level, where a well-defined peak is present (0.5–2.0 eV); the more extended and wide unoccupied band (above 2.0 eV) is instead mainly due to the unoccupied $5s$ and $5p$ states of Cd.

Comparing with the DOS of pure CdSe at the same Cd-Se bond length as in the spinel structure considered [dashed line in Fig. 2(a)], it is possible to notice a broadening of the valence band and the closing of the band gap due to the presence of the Cr *d* open shell (the lower density of states per cell is, of course, a result of the lower number of electrons in the CdSe cell with respect to the $CdCr_2Se_4$ cell).

Moreover, the spinel structure shows a lower hybridization between Cd 4*d* states and the higher valence band than the pure CdSe compound. In fact, in this latter case, the semicore Cd 4*d* states are found at lower binding energy than in the spinel structure.

B. Ferromagnetic calculation

In the ferromagnetic calculation the high instability present in the paramagnetic state is totally removed. This is clear from the total density of states plotted in Fig. 2(b): the Fermi level occurs in the middle of the Cr *d* states, in the gap between the bonding and antibonding *d* states, in agreement with what was found by Oguchi, Kambara, and Gondaira.[13] In Fig. 3 we plot the density of states projected on the different atomic sites for Cd, Cr, and Se (majority and minority contributions), respectively. These contributions, according to the usual definition, come from the states within the muffin-tin spheres. Contributions coming from the interstitial are included in the total DOS; we also point out that the valence states are mainly *p* and *d* states (and therefore well localized) and that we considered nearly touching spheres.

The main contribution to the valence band is due to the *d* states of Cr highly hybridized with the *p* states of Se. The states coming from Cd do not present any significant spin polarization, while a noticeable spin polarization is present on the Cr site: the states occupied (i.e., lying below the Fermi level) in the majority component are many more than the occupied states in the minority component. This will result in a large magnetic moment on the Cr site. As far as the Se-projected density of state is concerned, we notice that the shapes of the majority and minority components are quite similar and that there is not any energy shift among these states: this will result in a very small magnetic moment. As is clear from the plotted densities of states, the Cr *d* states lay on top of the Se *p* states and of the fundamental gap (Se *p* –Cd *s*) of CdSe; these states are highly hybridized with the states composing the valence band. Moreover, the exchange energy among the polarized Cr *d* states pushes the antibonding minority states towards higher energies, in the energy region of the Cd unoccupied *s* band and of the antibonding Se *p* states.

Relativistic interactions (i.e., spin-orbit effect), although changing and removing some degeneracy in the states, do not sensibly affect the composition of the resulting charge or the magnetic moment. The main result

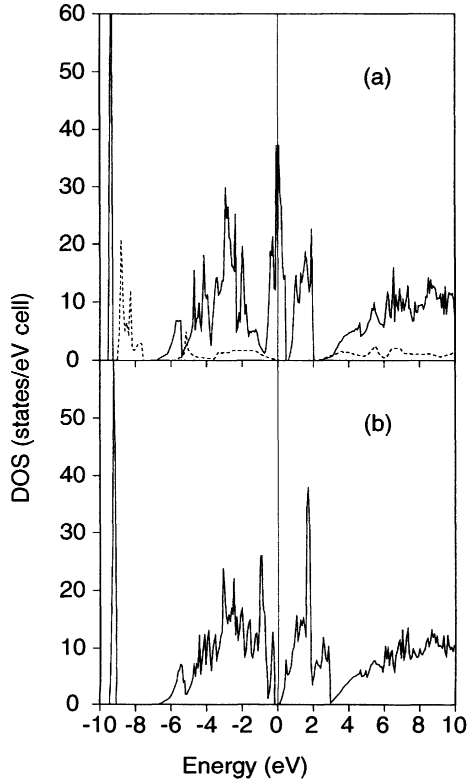

FIG. 2. (a) Total density of states for paramagnetic $CdCr_2Se_4$ (solid line) and CdSe (dashed line). (b) Total density of states for ferromagnetic $CdCr_2Se_4$.

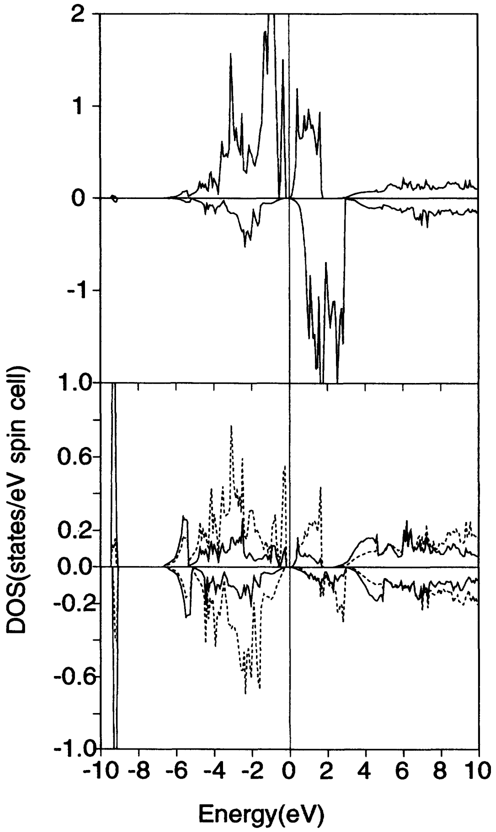

FIG. 3. Majority and minority component of the projected density of state for Cr (upper panel) and Cd and Se (lower panel), solid and dashed lines, respectively.

is to split levels in the conduction and valence bands with mainly Se *p* and Cd *d* character, while states with mainly Cr component are very little affected. The spin-orbit splitting at the top of the valence band (Se *p* states) is $\Delta^{so}=0.45$ eV, while the splitting for the Cr states is only $\Delta^{so}=0.01$ eV.

The valence band width (i.e., the separation at Γ between the low Se *s* states and the top of the Se *p* occupied states) is 14.0 eV, the same value as in pure CdSe at the same Cd-Se bond length as in the spinel structure. All the valence band is characterized by a large hybridization between Cr *d* and Se *p* states, the major contribution coming from the Cr *d* states localized in the region of 4 eV below the valence-band top.

We refer to photoemission results ranging from 10 to 50 eV (Refs. 11 and 9) in order to compare our calculated valence-band energies. The two previously mentioned experimental reports differ slightly in the main spectral features detected: they find a main peak at 1.45 (Ref. 11) or 1.30 (Ref. 9) eV below the valence-band maximum, and some other smaller features at 2.9 (Ref. 11) or 3.0 (Ref. 9) and at 5.25 (Ref. 11) or 5.29 (Ref. 9) eV. Miniscalco *et al.*[11] also report two features at lower binding energy: 5.85 and 10.7 eV, respectively. The exact position of the Cr *d* states is still now rather controversial and the object of discussion; comparing our theoretical results with the experiments we will try to clarify this issue.

The peak at higher binding energy (10.7 eV) is due to the Cd 4*d* contribution and it is related to the sharp peak at ~9.0 eV in our density of states; the energy position of the theoretical peak is shallower than the experimental finding, due to LDA which underestimates the exchange-correlation contribution in very confined corelike states.

The features at lower binding energies, on the other hand, relate rather well with features in the theoretical DOS. In particular, we can see that the peak at 1.45 (Ref. 11) or 1.30 (Ref. 9) eV, below the valence-band maximum, is in good correspondence with the huge peak in the partial density of states of Cr, due to a twofold degenerate Cr *d* state (majority-spin component) with symmetry Γ_{12}-E_g which presents a flat dispersion in proximity of the Brillouin-zone center. In this respect, our findings seem to agree more with the atomic-level-derived model proposed by Taniguchi, Fujimori, and Suga[9] than with the identification proposed by Miniscalco *et al.*[11] that attributes this state to a threefold degenerate T_{2g} Cr *d* state. According to our calculations, the Cr T_{2g}-$\Gamma_{25'}d$ state is much shallower in energy (we find this state at -0.79 eV). However, we should point out that in this energy region there are several Cr *d* bands and that the identification of the photoemission feature with one particular band is not straightforward.

We should notice that, in this energy region, minority-spin states should not contribute since they are mostly originating from Se *p* states and both photoemission experiments[9,11] seem to agree on the fact that the behavior of this feature as a function of the photon energy is characteristic of a *d*-like band (the experimental peak is enhanced as the photon energy is increased).

The other transitions found at binding energies 2.9, 5.25, and 5.85 eV also correspond to precise features in the calculated DOS. In particular, the transition at $\simeq 3.0$ eV is nicely located in the middle of the Se *p* band hybridized with the Cr *d* band, while features at higher binding energies (5.25 and 5.85 eV) seem to be located in the region where there is also a noticeable hybridization among Cr *d*, Se *p*, and the Cd *s* band.

The fundamental gap is usually referred to in the literature as the energy difference between the highest occupied *p* state in the valence band and the lowest unoccupied *s*-like state in the conduction band. According to our calculation, this energy gap is 2.38 eV (which is reduced to $\simeq 2.0$ eV, taking into account the spin-orbit splitting of the *p*-like valence top band) for the majority states and 3.08 eV for the minority states, while it is 0.79 eV in pure CdSe at the same Cd-Se bond length as in the spinel structure. In this same energy region are localized the unoccupied T_{2g} and E_g states of chromium.

Photoluminescence decay and quantum efficiency measurements have determined a fundamental gap of 1.8 eV, at 77 K.[20] This result agrees with a previously detected luminescence transition at 1.8 eV, which has been attributed to transitions between Cr states split by crystal-field and excited states[21] (and therefore not directly related to the fundamental band gap as previously defined); however, we should notice that photoluminescence experiments tend to include shallow impurity effects in the optical transition and therefore this transition may not correspond to the fundamental band gap.

In Table I we report the decomposition of the total muffin-tin charge into different angular momentum components. As it is possible to observe, the total charge obtained from the paramagnetic calculation corresponds, exactly, to the sum of the majority and minority components in the ferromagnetic calculation. Also, with the exception of the Cr atom, the total paramagnetic charge is equally distributed between the two different spin components, showing that the net spin polarization on the Cd

TABLE I. Decomposition of the total muffin-tin charge into different angular momentum components for the different cases considered. The symbols PM and FM stand for paramagnetic and ferromagnetic calculation, respectively.

Atom	Q_s	Q_p	Q_d	Q_{tot}
		PM		
Cd	0.44	0.35	9.32	10.12
Cr	0.22	0.23	3.95	4.41
Se	1.55	2.61	0.05	4.22
		FM (majority)		
Cd	0.22	0.17	4.66	5.06
Cr	0.13	0.13	3.39	3.66
Se	0.77	1.28	0.03	2.08
		FM (minority)		
Cd	0.21	0.17	4.67	5.06
Cr	0.10	0.11	0.53	0.74
Se	0.77	1.38	0.02	2.17

TABLE II. Total magnetic moment μ [in Bohr magneton (μ_B)] per atom and its decomposition into different angular momentum components, on the different atomic species for the ferromagnetic calculation.

Atom	μ_s	μ_p	μ_d	μ_T
Cd	0.02	0.00	0.00	0.02
Cr	0.03	0.02	2.86	2.91
Se	0.00	−0.1	0.01	−0.09

and Se atoms is very low.

This is even more clear in Table II where the magnetic moments per atom and per angular momentum contributions (within the muffin-tin spheres) are shown. The magnetic moment is very low on the Cd atom which does not really contribute to the states on the valence-band top; the Cr atom, on the other hand, shows a larger polarization (its magnetic moment is a little less than $3\mu_B$), most of its spin polarization coming from the *d* states. The contribution coming from the interstitial region is as large as $0.5\mu_B$ per formula unit, probably mainly due to the Cr *d* states. This result seems in qualitative agreement with the schematic picture given by Taniguchi, Fujimori, and Suga,[9] obtained considering the hybridization among Cr 3*d* and Se 4*p* states, and, if the contribution from the interstitial is considered, also with previous *X*-α calculations by Oguchi, Kambara, and Gondaira[13] which give $\mu_{\text{Cr}}=3.5\mu_B$. In agreement with the previously mentioned calculation and with some NMR experimental results[22], we find that the Se atom shows an antiparallel alignment with respect to the Cr *d* shell, resulting in a negative and low magnetic moment (mainly due to the Se 4*p* shell, hybridized with the Cr 3*d* shell). This is also shown by the total spin density (obtained by subtracting the total minority charge from the total majority charge density) projected on the [110] plane and shown in Fig. 4. The regions with antiparallel spin are localized in proximity of the Se atoms: this is reasonably explained by the exchange interaction among hybridized Cr *d* states and Se *p* states: there is an "attraction" among orbitals with parallel spin, while orbitals with opposite spins are repelled in more distant regions.

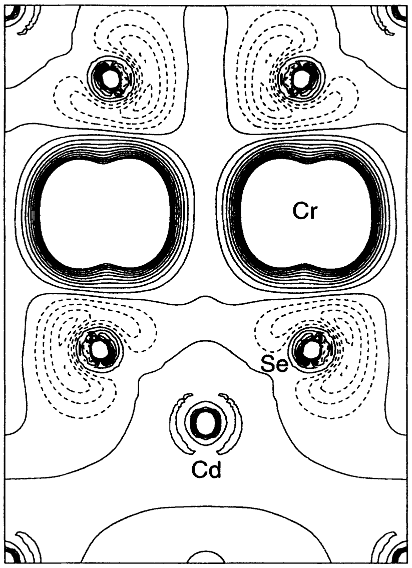

FIG. 4. Total spin density (dashed lines correspond to antiparallel spin density contours) of $CdCr_2Se_4$ in the (110) plane. Levels are given in units of 2 electrons/cell.

CONCLUSIONS

First-principles methods have been used to investigate the electronic properties of the magnetic spinel $CdCr_2Se_4$ in its paramagnetic and ferromagnetic phases. The relativistic FLAPW method has been able to identify the role of the Cr 3*d* electrons in the chemical bonding. The projected density of states compares very well, for the majority- and minority-spin orientations, with the photoemission studies. A well-defined assignment of the intragap transition has been obtained with a detailed analysis of the crystal-field splittings due to the empty Cr *d* states. The presence of different cations with noncomplete shells produces effects notably relevant when compared to the electronic scheme of the nonmagnetic binary CdSe compound. The total muffin-tin charge is analyzed through the angular momentum components accounting for the different polarizability of the cations in the ternary. The previous theoretical models obtained in a non-first-principles calculation have been analyzed and compared sometimes favorably with the present *a priori* results. The exact definition of the energy dispersion is now a step toward a detailed analysis of the structural modifications induced by different cations and by noncomplete electronic shells in this interesting class of magnetic ternary spinels.

ACKNOWLEDGMENTS

This work has been partially supported by the Italian Consiglio Nazionale delle Ricerche CNR through the Progetto Finalizzato, Grant No. 89.00006-69.

---

[1] As a general reference, see *Proceedings of the 7th International Conference on Ternary and Multinary Compounds,* edited by S. K. Deb and A. Zunger (Materials Research Society, Pittsburgh, 1987), and *Proceedings of the 8th International Conference on Ternary and Multinary Compounds,* edited by S. I. Radautsan and C. Schwab (Shtiintsa Press, Kishinev, 1992).

[2] T. de Pascale, M. Marinelli, F. Meloni, G. Mula, M. Serra, A. Borghesi, G. Guizzetti, and L. Nosenzo, in *Atomic Scale Calculations in Material Science,* edited by J. Tersoff, D. Vanderbilt, and V. Vitek, MRS Symposia Proceedings No. 141 (Materials Research Society, Pittsburgh, 1989), p. 195.

[3] M. Marinelli, T. De Pascale, F. Meloni, G. Mula, and M. Serra, Phys. Scr. **39**, 343 (1989).

[4] M. Marinelli, S. Baroni, and F. Meloni, Phys. Rev. B **38**, 8528 (1988).

[5] A. Baldereschi and F. Meloni, Jpn. J. Appl. Phys. **19**, 161

(1980).

[6] M. Marinelli, T. de Pascale, F. Meloni, G. Mula, M. Serra, and S. Baroni, Phys. Rev. B **40**, 1725 (1989).

[7] J. E. Bernard and A. Zunger, Phys. Rev. B **37**, 6835 (1988).

[8] E. F. Steigmeier and G. Harbeke, Phys. Kondens. Mater. **12**, 1 (1970).

[9] M. Taniguchi, A. Fujimori, and S. Suga, Solid State Commun. **70**, 191 (1989).

[10] H. J. F. Jansen and A. J. Freeman, Phys. Rev. B **30**, 561 (1984).

[11] W. J. Miniscalco, B. C. McCollum, N. G. Stoffel, and G. Margaritondo, Phys. Rev. B **25**, 2947 (1982).

[12] P. K. Baltzer, H. W. Lehmann, and M. Robbins, Phys. Rev. Lett. **15**, 493 (1965).

[13] T. Oguci, T. Kambara, and K. I. Gondaira, Phys. Rev. B **22**, 872 (1980).

[14] L. Hedin and B. I. Lundqvist, J. Phys.C **4**, 2064 (1971).

[15] U. von Barth and L. Hedin, J. Phys. C **5**, 1629 (1972).

[16] D. D. Koelling, Solid State Commun. **53**, 1019 (1985).

[17] A. H. MacDonald, W. E. Pickett, and D. D. Koelling, J. Phys. C **13**, 2675 (1980).

[18] A. Baldereschi, Phys. Rev. B **7**, 5212 (1973); D. J. Chadi and M. L. Cohen, *ibid.* **8**, 5747 (1973); H. J. Monkhorst and J. P. Pack, *ibid.* **13**, 5188 (1976).

[19] J. Rath and A. J. Freeman, Phys. Rev. B **11**, 2109 (1975); O. Jepsen and O. K. Anderson, Solid State Commun. **9**, 1763 (1971); G. Lehman and H. Taut, Phys. Status Solidi **54**, 469 (1972).

[20] S. S. Yao, F. Pellegrino, R. R. Alfano, W. J. Miniscalco, and A. Lempicki, Phys. Rev. Lett. **46**, 558 (1981).

[21] V. G. Veselago, Colloq. Int. C. N. R. S. **242**, 295 (1974).

[22] S. B. Berger, J. I. Budnik, and T. J. Burch, J. Appl. Phys. **39**, 658 (1968).